Available online at www.sciencedirect.com
SCIENCE DIRECT®
Journal of Electron Spectroscopy and Related Phenomena 137–140 (2004) 595–599
JOURNAL OF ELECTRON SPECTROSCOPY and Related Phenomena
www.elsevier.com/locate/elspec

Electronic structure and large thermoelectric power in $Ca_3Co_4O_9$

T. Takeuchi [a,*], T. Kondo [b], K. Soda [b], U. Mizutani [b], R. Funahashi [c], M. Shikano [c], S. Tsuda [d], T. Yokoya [d], S. Shin [d], T. Muro [e]

[a] *Research Center for Advanced Waste and Emission Management, Nagoya University, Nagoya 464-8603, Japan*
[b] *Department of Crystalline Materials Science, Nagoya University, Nagoya 464-8603, Japan*
[c] *National Institute of Advanced Industrial Science and Technology Kansai, Ikeda 563-8577, Japan*
[d] *Institute of Solid State Physics, University of Tokyo, Kashiwa 277-8581, Japan*
[e] *Japan Synchrotron Radiation Research Institute, Hyogo 679-5198, Japan*

Available online 18 March 2004

Abstract

Resonant photoemission spectroscopy, soft X-ray emission spectroscopy, soft X-ray absorption spectroscopy, and high-resolution ($\Delta E \approx 10$ meV) ultraviolet photoemission spectroscopy were performed on a layered cobalt oxide, $Ca_3Co_4O_9$, which has attracted interests as one of the potential thermoelectric materials because of its possession of high thermoelectric power S, relatively low electrical resistivity ρ, and small thermal conductivity κ. A narrow band of 1.5–2 eV in width was observed in the photoemission spectra with its center at 1.0 eV below the Fermi level (E_F). This peak turns out to be less significant when Co 2p–3d resonance takes place, indicating that it consists mainly of O 2p and of small amount of Co 3d component. Since E_F is located near the high-energy edge of this narrow band, the density of states at E_F is finite but negligibly small at room temperature. An energy-gap across E_F opens below 50 K with decreasing temperature. This development of the energy-gap causes the insulating behavior; divergence both in electrical resistivity and Hall coefficient. We calculated thermoelectric power $S(T)$ using the photoemission spectra near E_F. The calculated $S(T)$ shows almost half of the measured value. Large thermoelectric power up to 200 μV/K observed for the $Ca_3Co_4O_9$ is closely related to the metallic electron transport in a less dispersive band with E_F near its band-edge.

Keywords: Thermopower; Cobalt oxide; UPS; RPES; XAS; XES

1. Introduction

A large thermoelectric figure of merit $Z = (S^2\sigma)/\kappa$, that is known as a necessity of practical thermoelectric materials, requires a large thermoelectric power S, a large electrical conductivity σ, and a small thermal conductivity κ. Thermoelectric power as well as the electrical conductivity is a function of carrier concentration. These two quantities show opposite carrier concentration dependence; thermoelectric power increases while electrical conductivity decreases with decreasing carrier concentration [1]. It has been widely believed, therefore, that there is an optimal condition of the carrier concentration at about $10^{19}\,cm^{-3}$ that provides the largest thermoelectrical figure of merit Z. In this respect, doped semiconductors, such as Bi_2Te_3, SiGe, PbTe, and so on, have been employed as thermoelectric devices and their performance has been discussed in terms of carrier concentration [1].

Recently, thermoelectric power in a layered cobalt oxide $NaCoO_2$, which is characterized by a CoO_2 triangular-lattice layer consisting of edge-shared CoO_6 octahedrons, were reported to exceed 80 μV/K at room temperature even though its electrical resistivity stays below 200 μΩ cm at room temperature [2,3]. This was surprising fact because contradicting two conditions, large thermoelectric power and metallic conductivity, are simultaneously achieved in this cobalt oxide. Its high temperature stability further promoted us to utilize the $NaCoO_2$ as a thermoelectric device.

More recently, it was reported that other layered cobalt oxides, such as $(Ca_2CoO_3)_4(CoO_2)_6$ (abbreviated as $Ca_3Co_4O_9$), $Bi_2Sr_3Co_2O_9$, and $Tl_{0.4}(Sr_{0.9}O)_{1.12}CoO_2$, also possess a large thermoelectric power and a metallic electronic conductivity [4–8]. The structures in these cobalt oxides are characterized by a CoO_2 triangular-lattice layer as well as that in the $NaCoO_2$. These facts let us believe that the large thermoelectric power with metallic electrical

* Corresponding author. Tel.: +81-52-789-5620; fax: 81-52-789-3724.
E-mail address: takeuchi@nuap.nagoya-u.ac.jp (T. Takeuchi).

0368-2048/$ – see front matter © 2004 Elsevier B.V. All rights reserved.
doi:10.1016/j.elspec.2004.02.013

conductivity is characteristic of the CoO_2 triangular-lattice layer.

In addition to its large thermoelectric power and the metallic electronic conductivity preferable for a thermoelectric devices, $Ca_3Co_4O_9$ shows a low thermal conductivity most likely associated with the misfit structure between the CoO_2 layer and the Ca_2CoO_3 rock-salt layer [9]. As a result of the small thermal conductivity, figure of merit in $Ca_3Co_4O_9$ exceeds $ZT = 0.87$ at 973 K [8]. It is, therefore, regarded as one of the most promising candidates for the practical thermoelectric material.

Beside its practical application, the physical mechanism leading the large thermoelectric power in these layered cobalt oxides has been a point of controversy in condensed matter physics. Koshibae et al. proposed a theory for the large thermoelectric power in cobalt oxides on the basis of Hikes formula [10]. In their theory, degeneracy in the cobalt 3d states plays an important role in enhancing the thermoelectric power through their large configurational entropy. Unfortunately, however, it does not explain the metallic electrical conductivity with a negative temperature coefficient that is one of the typical properties in the layered cobalt oxides.

The effect of the electron correlation in these layered cobalt oxide has been also attracted interest, because coherent–incoherent transition was clearly observed in a high-resolution angle resolved photoemission spectroscopy measurement [11]. If strong electron correlation takes place, the electron transport properties, such as σ and S, would be crucially affected by it. Since photoemission spectra are sensitive to the electron correlation, it is of importance to discuss the electron transport properties in terms of the photoemission spectra near the Fermi level (E_F).

In this paper, the electronic structure in $Ca_3Co_4O_9$ is investigated in detail using photoemission spectroscopy and soft X-ray emission and absorption spectroscopy. The electron transport properties, σ and S, are discussed in terms of the electronic structure near E_F. By calculating $S(T)$ from a measured spectrum with assumption of metallic electron conduction, we will discuss the origin of the large thermoelectric power in the layered cobalt oxides.

2. Experimental procedure

High-quality single crystals were grown by the flux method. The details of the sample preparation were reported elsewhere [8]. Bulk-sensitive Co 2p–3d resonant photoemission spectroscopy (RPES) measurements with incident photon energies of $h\nu = 775$–780 eV were performed in the beam line BL25SU at the third generation 8 GeV synchrotron radiation facility SPring-8, Hyogo, Japan. The energy resolution of the RPES measurements was better than 120 meV, which was determined as the energy width of the intensity-reduction from 90 to 10% at the Fermi edge of the reference gold electrically contacting with the measured samples.

HeIα photoemission spectroscopy (UPS) measurements with an energy resolution of 10 meV were also performed in ISSP, The University of Tokyo, in order to determine the electronic structure near E_F in detail. We used Gammadata-Sicenta SES2002 hemispherical analyzer in both RPES and UPS measurement. The clean and flat surfaces were obtained by cleaving samples under the ultra-high vacuum condition of a base pressure better than 10^{-11} Torr. Since no significant angle dependence was observed in both RPES and UPS measurements, the cleaved surfaces were expected to have roughness that obscure angle dependence of the photoelectron intensity.

Co 2p–3d soft X-ray absorption spectroscopy (XAS) measurements were performed in the BL19B in the Photon Factory, KEK, Japan. We used bulk sensitive fluorescence yield method for the present XAS measurement. Soft X-ray emission spectroscopy associated with Co 2p–3d transition was also measured at room temperature using the electron probe micro-analyzer (Shimadzu EPMA1400).

3. Results

Fig. 1(a) shows the Co 2p–3d on-resonant photoemission spectrum measured at $h\nu = 778.3$ eV together with the off-resonant one at $h\nu = 771$ eV in Fig. 1(b). The Co 2p–3d X-ray absorption spectrum is shown in Fig. 1(c). Five different structures, each of which corresponds to bands, in the off-resonant spectrum are marked with A–E at binding energies (B.E.) = 1.0, 2.9, 3.5, 5.0, and 6.2 eV, respectively. When the Co 2p–3d resonance takes place, all bands except for D drastically develops. The valence band in the $Ca_3Co_4O_9$ is composed only of Co 3d and O 2p electrons, and the bands that have the Co 3d component must be enhanced at the Co 2p–3d resonance. Therefore, the hump-structure denoted as D in Fig. 1(b) is safely assigned as non-bonding O 2p bands because it disappeared at the Co 2p–3d resonant.

An intense peak observed at 1.0 eV below E_F in the off-resonant spectrum turned out to be less obvious in the on-resonant spectrum, though the intensity at that energy increased more than 10 times larger with the Co 2p–3d resonance. The Co 2p–3d SXES spectrum, that reflects Co 3d partial density of states, has small intensity at B.E. = 1.0 eV in sharp contrast to the large intensity at B.E. = 3.0–8.0 eV, where bands B, C, and E lie. We assigned that the band(s) at 1.0 eV below E_F consists mainly of O 2p and of a minor amount of Co 3d component.

Note here that E_F is located at the high-energy edge of this narrow band(s) centered at 1.0 eV. The density of states at E_F ($N(E_F)$) is fairly small but finite. The electrical resistivity in the $Ca_3Co_4O_9$ at high temperature above 200 K was reported to have a positive temperature coefficient, that is a typical behavior of metals. This metallic behavior in the electrical

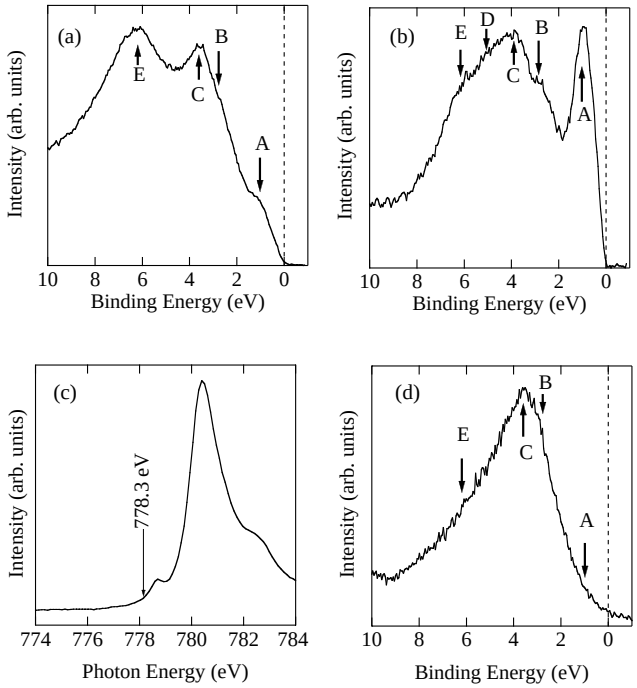

Fig. 1. (a) Co 2p–3d RPES spectrum of the $Ca_3Co_4O_9$ measured with $h\nu = 778.3$ eV at 20 K. Four humps marked with A–C, and E are observed at 1.0, 2.9, 3.5, and 6.2 eV, respectively. (b) XPS spectrum measured with $h\nu = 771$ eV at 20 K. A small hump marked as D is observed at 5.0 eV in addition to the humps that enhanced in the RPES spectrum. (c) Co 2p–3d absorption spectrum at 20 K. The photon energy of $h\nu = 778.3$ eV was used for the RPES measurement. This energy was selected to avoid getting affected by the Auger electrons. (d) Co 2p–3d emission spectrum measured at room temperature. Although rather poor energy resolution ($\Delta E \sim 1$ eV) obscured fine structures in the spectrum, humps marked as A–C, and E can be observed as that in the RPES spectrum. Sharp peak in XPS spectrum at 1.0 eV and rather small peaks in RPES and SXES spectra at the same energy indicate that the amount of Co 3d component in the band 1.0 eV below E_F is much smaller than the component of O 2p. Vertical broken lines in (a), (b), and (d) indicate the Fermi level.

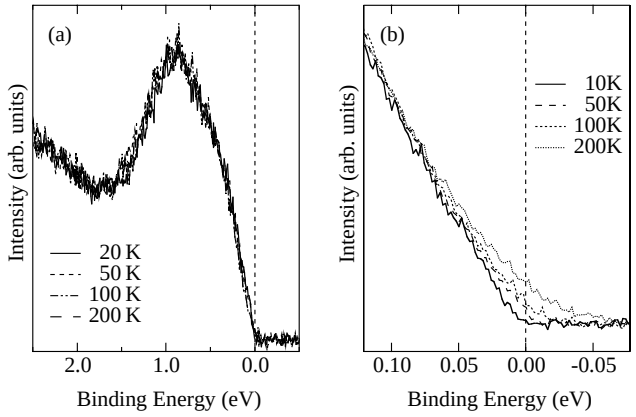

Fig. 2. (a) XPS spectra measured with a incident energy of $h\nu = 778.3$ eV at 20, 50, 100, and 200 K. Spectrum shape is almost temperature independent. (b) High-resolution HeIα UPS spectra measured at 10, 50, 100, and 200 K. At temperature above 50 K, density of states at E_F is kept finite indicating a metallic state. An energy-gap of about 15 meV form E_F opens below 50 K. Drastically increasing electrical resistivity and Hall coefficient with decreasing temperature below 50 K are accounted for by considering this gap-generation across E_F.

conduction must be introduced by the finite density of states at E_F.

The electrical resistivity, however, drastically increases with decreasing temperature below 100 K [4]. In order to investigate the relation between the electrical resistivity and the electronic structure in the $Ca_3Co_4O_9$, high-resolution UPS measurement was performed and the electronic structure in the vicinity of E_F was revealed. XPS spectra measured at 20, 50, 100, and 200 K are shown in Fig. 2(a), and UPS spectra near E_F measured at 20 K, 50 K, 100 K, and 200 K are in Fig. 2(b). Although XPS spectra show no significant temperature dependence, UPS spectra of high-energy resolution clearly indicates that $N(E_F)$ decreases with decreasing temperature and turns out to have almost no intensity at 20 K. An increase in electrical resistivity and Hall coefficient below 50 K with decreasing temperature [4,6] must be caused by the development of this energy-gap across E_F through decreasing number of conducting electrons.

The gap width is estimated to be <20 meV at 10 K, that is too small to be revealed by the XPS or RPES measurement of the energy resolution of 120 meV. High-energy resolution of the present UPS measurement played an essential role in investigating the gap development at low temperature. The increase in the electrical resistivity with decreasing temperature would not be fitted by the equation for the thermal excitation across a rigid band gap [4]. That is because the energy-gap shows strong energy dependence as we observed in the present UPS measurement. To fully understand the temperature dependence of the electrical resistivity below 50 K, further quantitative analysis to reveal the temperature dependence of the energy-gap is required.

The origin of the energy-gap development across E_F is not clear now. It should be commented here, however, that the development of a spin density wave (SDW) below 100 K was observed in the μSR measurement [12]. This development of SDW may cause an energy-gap due to a nesting of the Fermi surface(s). Another candidate for the gap-generation mechanism is that associated with the electron–electron correlation. Theoretical studies on a triangular lattice with strong electron correlation predicted the development of spin density wave and energy-gap even without a nesting of the Fermi surface [13–15]. The coherent–incoherent transition, that is one of the typical phenomena in the system under the stong electron correlation, was observed by the angle resolved UPS measurements for other layered cobalt oxides. This fact may indicate the importance of electron correlation in this system. We should note, however, that any evidence for the coherent–incoherent transition was not observed in the present high-resolution UPS measurement. Thus, we consider that the nesting of the Fermi surface is responsible for the energy-gap generation in the $Ca_3Co_4O_9$. High-energy resolution angle resolved photemission spectroscopy with high-quality samples would provide us a clear interpretation for this problem.

4. Discussion

In this section, the origin of the high thermoelectrical power observed on the $Ca_3Co_4O_9$ is discussed. On the basis of the Boltzmann transport equation, the thermoelectric power $S(T)$ in a metallic system can be deduced by the following formula as a function of temperature.

$$S(T) = \frac{1}{eT}\frac{\int_{-\infty}^{\infty}\sigma(\varepsilon)(\varepsilon-\mu)(\partial f(\varepsilon)/\partial\varepsilon)\,\mathrm{d}\varepsilon}{\int_{-\infty}^{\infty}\sigma(\varepsilon)(\partial f(\varepsilon)/\partial\varepsilon)\,\mathrm{d}\varepsilon} \quad (1)$$

Here, $\sigma(\varepsilon)$ represents the contribution of electrons at ε to the electrical conductivity. $f(\varepsilon)$ and μ denote the Fermi–Dirac distribution function and the chemical potential, respectively. Since $\partial f(\varepsilon)/\partial\varepsilon$ has a finite value only in an energy range of a few k_BT in width centered at the chemical potential μ, it is very important to know $\sigma(\varepsilon)$ in this energy range.

If we assume an isotropic system, $\sigma(\varepsilon)$ was calculated by:

$$\sigma(\varepsilon) = \frac{e^2A(\varepsilon)v(\varepsilon)\tau(\varepsilon)}{12\pi^3\hbar} = \frac{e^2}{3}v(\varepsilon)^2\tau(\varepsilon)N(\varepsilon), \quad (2)$$

where $A(\varepsilon)$, $v(\varepsilon)$, $\tau(\varepsilon)$ and $N(\varepsilon)$ represent the area of equienergy surface, group velocity, relaxation time, and density of states, respectively. The energy range to be considered in the integration in Eq. (1) is very narrow because of the energy range in which finite magnitude in the $\partial f(\varepsilon)/\partial\varepsilon$ exists. Thus, we assume here an energy independent group velocity and an energy independent relaxation time. Eq. (1) is transformed into:

$$S(T) = \frac{1}{eT}\frac{\int_{-\infty}^{\infty}N(\varepsilon)(\varepsilon-\mu)(\partial f(\varepsilon)/\partial\varepsilon)\,\mathrm{d}\varepsilon}{\int_{-\infty}^{\infty}N(\varepsilon)(\partial f(\varepsilon)/\partial\varepsilon)\,\mathrm{d}\varepsilon}. \quad (3)$$

We substituted UPS spectra for the $N(\varepsilon)$ in Eq. (3) to deduce the thermoelectric power $S(T)$ in the $Ca_3Co_4O_9$. In order to get information about the conduction band just above E_F, room temperature USP spectrum divided by $f_{RT}(\varepsilon)$ was employed. This method is valid only if the energy resolution of the measurement is much better than the thermal broadening of k_BT. The resulting spectrum is shown in Fig. 3. We compensated the conduction band in the high-energy range by the extrapolating the spectrum. Three different models, which were used in the calculation of $S(T)$, are also superimposed on the spectrum in Fig. 3.

One may wonder that the unit of the UPS intensity is different form that of $N(\varepsilon)$ and that it cannot be used as a substitute for $N(\varepsilon)$. We note here, however, that the dimension in $N(\varepsilon)$ is canceled in Eq. (3) because it exists both in the denominator and numerator. The calculated $S(T)$ curves are shown in Fig. 4 together with the reported ones [4,8]. Though its absolute value is kept only half of the measured ones, the calculated $S(T)$ is qualitatively consistent with the measured one, in possessing a positive temperature dependence and high values exceeding 100 μV/K at high temperature above 600 K.

We conclude that the large thermoelectric power observed for the $Ca_3Co_4O_9$ is closely related to the metallic electron transport in a unique electronic structure characterized by a narrow band width of <2 eV and E_F near its band edge. The difference between the measured $S(T)$ and calculated one may arise from the assumption of energy independent group velocity and relaxation time.

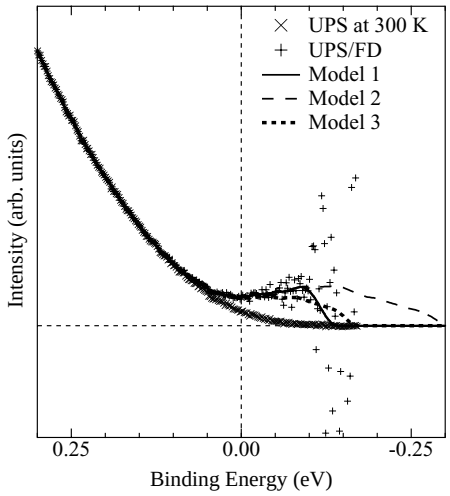

Fig. 3. UPS spectrum of $Ca_3Co_4O_9$ measured at room temperature and that divided by the Fermi–Dirac distribution function (UPS/FD). Information about the density of states above E_F can be observed in the UPS/FD spectrum up to B.E. = −0.1 eV, that is about $4k_BT$ above E_F. Three models of density of states above E_F were constructed and superimposed on the UPS spectrum.

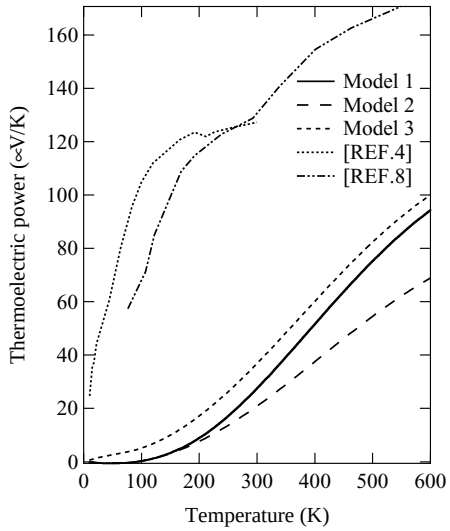

Fig. 4. Thermoelectric power $S(T)$ calculated from UPS spectrum on the basis of the Boltzmann transport equation. The measured $S(T)$ [4,8] were superimposed. A positive temperature coefficient in the thermoelectric power was confirmed in the simulations as well as that in the experiments.

5. Conclusion

The valence band electronic structure in the $Ca_3Co_4O_9$ of one of potential thermoelectric materials was determined

by combining the bulk-sensitive RPES and high-resolution UPS measurements. The electronic structure near E_F is characterized by a narrow band of <2 eV in width and the location of E_F near its edge. By calculating $S(T)$ from the measured UPS spectrum, we conclude that this unique electronic structure and metallic electron transport are closely related to the co-existence of the large thermoelectric power and the relatively low electrical resistivity.

References

[1] G. Mahan, B. Sales, J. Sharp, Phys. Today 50 (1997) 42.
[2] I. Terasaki, Y. Sasago, K. Uchinokura, Phys. Rev. B56 (1997) R12685.
[3] K. Fujita, T. Mochida, K. Nakamura, Jpn. J. Appl. Phys. 40 (2001) 4644.
[4] A.C. Masset, C. Michel, A. Maignan, M. Hervieu, O. Toulemonde, F. Studer, B. Raveau, J. Hejtmanek, Phys. Rev. B 62 (2000) 166.
[5] R. Funahashi, I. Matsubara, H. Ikuta, T. Takeuchi, U. Mizutani, S. Sodeoka, Jpn. J. Appl. Phys. 39 (2000) L1127.
[6] R. Funahashi, I. Matsubara, H. Ikuta, T. Takeuchi, U. Mizutani, Mat. Trans. 42 (2001) 956.
[7] S. Hébert, S. Lambert, D. Pelloquin, A. Maignan, Phys. Rev. B 64 (2001) 171201-1
[8] M. Shikano, R. Funahashi, Appl. Phys. Lett. 82 (2003) 1851.
[9] Y. Miyazaki, M. Onoda, T. Oku, M. Kikuchi, Y. Ishii, Y. Ono, Y. Morii, T. Kajitani, J. Phys. Soc. Jpn. 71 (2002) 495.
[10] W. Koshibae, K. Tsutsui, S. Maekawa, Phys. Rev. B 62 (2000) 6869.
[11] T. Valla, D.P. Jhonson, Z. Yusof, B. Wells, Q. Li, M.S. Loureiro, R. Cava, M. Mikami, Y. Mori, M. Yoshimura, T. Sasaki, Nature 417 (2002) 627.
[12] A. Kawabata, Solid State Commun. 38 (1981) 823.
[13] R.H. Krishnamurthy, C. Jayaprakash, S. Saker, W. Wenzel, Phys. Rev. Lett. 64 (1990) 950.
[14] M. Fujita, M. Ishimura, K. Nakao, J. Phys. Soc. Jpn. 60 (1991) 2831.
[15] M. Fujita, T. Nakanishi, K. Machida, Phys. Rev. B45 (1992) 2190.